Article

Optimization of the Alkali-Silane Treatment of *Agave lechuguilla* Fibers (Ixtle) for Potential Reinforcement in Polymeric Composites

Noemi Jardon-Maximino [1], Mariamne Dehonor Gómez [2], Rolando Villa Moreno [2], M. D. Baeza-Alvarado [2] and Luis Edmundo Lugo Uribe [2,*]

[1] CONAHCYT—CIATEQ, A.C. Centro de Tecnología Avanzada, Lerma 52004, Estado de México, Mexico; noemi.jardon@ciateq.mx
[2] CIATEQ, A.C. Centro de Tecnología Avanzada, Lerma 52004, Estado de México, Mexico; mariamne.dehonor@ciateq.mx (M.D.G.); rolando.vmoreno@ciateq.mx (R.V.M.); maria.baeza@ciateq.mx (M.D.B.-A.)
* Correspondence: luis.lugo@ciateq.mx

Abstract: Reinforced polymeric composites with natural fibers have garnered significant interest in recent years due to the need for biomass utilization and the requirements of various industries, such as automotive and construction. Among these natural fibers, *Agave lechuguilla* fiber, commonly known as ixtle (FIx) or Tampico fiber, exhibits important characteristics such as length, high strength, and durability. However, there is limited literature on its conditioning, functionalization, and utilization as a reinforcing material in polymeric composites (CP). This study presents the optimization of the alkali-silane treatment of FIx, identifying the most suitable reaction conditions to enhance their thermal stability, tensile strength, and silane coupling agent (ACSi) grafting on the fiber surface. The chemical treatment with ACSi proved highly effective, resulting in a significant grafting content, which was confirmed through FTIR and SEM–EDS analyses. The high level of functionalization did not compromise the mechanical performance of the fibers, suggesting that functionalized FIx holds great potential as a reinforcing material in CP. These findings open new paths for the sustainable use of *Agave lechuguilla* fibers, contributing to the development of environmentally friendly and high-performance polymeric composites in various industrial applications.

Keywords: *Agave Lechuguilla*; natural fiber; silane coupling agent

1. Introduction

Polymeric composites (PC) based on natural fibers (NFs) have emerged as materials of interest in the packaging, automotive, and construction industries [1–6]. NFs offer attractive advantages over synthetic fibers, as they are biodegradable reinforcing agents, non-abrasive to processing equipment, and their low density, along with suitable strength and stiffness, make them promising candidates for reinforcing polymeric matrices [3–5].

Agave lechuguilla has a wide natural distribution in the Mexican territory (central and northern regions) [7–11]. From pre-Hispanic times to the present day, various Mexican communities have engaged in the production of diverse products based on ixtle fibers (FIx). The production process mainly involves fiber extraction, washing, drying, spinning, and weaving [8,12,13]. However, the practice of these techniques has significantly declined due to the introduction of plastic materials in products where this fiber was once used, adversely affecting the ixtle industry.

The most studied NFs extracted from agave in PC are those from *Agave fourcroydes* (henequen), *Agave sisalana* (sisal), *Agave tequilana* Weber (blue agave), and, to a lesser extent, *Agave Angustiofolia*, and *Agave Americana* [1,2,6,14–17].

To the best of our knowledge, only a few studies have focused on the conditioning and use of FIx as reinforcement in PC [18–22]. FIx exhibits tough physical and mechanical

properties and is resistant to chemical solvents, suggesting its potential as a reinforcement for polymeric matrices [13,23].

The chemical composition of NFs, including cellulose, lignin, hemicellulose, pectins, waxes, and mineral salts, among others, depends on factors such as soil type, moisture, and nutrients in the plant's growing environment. Furthermore, the chemical composition of NFs influences their thermal and mechanical properties. For instance, the tensile strength and Young's modulus of NFs are influenced by the cellulose content and its degree of crystallinity, while a higher hemicellulose content increases the moisture absorption capacity of NFs [24]. However, NFs possess some disadvantages, such as their hydrophilicity, stemming from the hydroxyl groups in cellulose and hemicellulose, which leads to incompatibility with hydrophobic polymeric matrices. This results in poor interfacial adhesion and, consequently, inferior mechanical properties of the PC [14,25]. Additionally, variables such as the concentration and size of the NF, as well as the PC preparation method, also influence its mechanical properties.

Various methods have been employed to enhance the compatibility between NF and polymeric matrices by promoting interfacial interactions. These methods involve incorporating a third component (compatibilizer) or modifying the NF surface through chemical treatments. Certain chemical treatments aim to remove impurities, increase roughness, or reduce the hydrophilic characteristics of the NF surface. Moreover, it has been reported that chemical treatments can alter the mechanical and thermal properties of NFs [26].

Alkaline treatment has been reported to modify the structure and chemical composition of NFs. Several studies have demonstrated that this treatment enhances the performance of NFs as reinforcement in PCs, as it is one of the most effective methods for modifying the NF surface. This process allows for the removal of impurities and hemicellulose, resulting in increased thermal stability and surface roughness [14,25]. The effectiveness of the alkaline treatment is influenced by parameters such as NaOH concentration, temperature, time, and the weight ratio of NF in the solution [25]. An increase in NaOH concentration has been reported to elevate the cellulose content while reducing the hemicellulose and lignin contents [27]. Typically, at high NaOH concentrations and temperatures, more hemicellulose and lignin are removed, enabling greater interaction between cellulose microfibrils through hydrogen bonding [28]. Consequently, this leads to a reduction in diameter and an increase in tensile strength of NFs, both of which are desirable traits in NF intended for use as reinforcement in PC [29].

Grafting reactions of NFs with silane coupling agents (ACSi) have been extensively reported as a chemical method for functionalizing NFs. ACSi can react with the hydroxyl groups present on the surface of NFs as well as the functional groups of certain polymeric matrices. ACSi have a structure of R(4-n)-Si-(R'X)n (*n* = 1, 2), where R is an alkoxy, X represents a functionality, and R' is an alkyl spacer [30]. In an aqueous environment, the hydrolysable alkoxy groups of silanes can react with the hydroxyl groups of NFs, forming stable bonds. The mechanism proposed by various authors proceeds through four stages: (1) hydrolysis—the silane hydrolyzes in the presence of water and a catalyst (acid or base), releasing alcohol and producing reactive silanol groups; (2) self-condensation—condensation of the silanol groups takes place; (3) adsorption—the reactive silanol monomers or their oligomers are physically adsorbed onto the hydroxyl groups on the NF surface through hydrogen bonds; and (4) grafting—hydrogen bonding between silanol and hydroxyl groups of NFs can be converted into a covalent bond (-Si-O-Si), releasing water [30,31].

Most of the ACSi used in the treatment of NFs are trialkoxysilanes. As for functional groups, they typically include alkyl, amino, mercaptan, vinyl, or methacryloxy groups [30]. ACSi with amino functionality are the most reported in PC formulated with thermoplastics and NFs. ACSi with vinyl and methacryloxy functionality are able to form covalent bonds with polymeric matrices in the presence of peroxide initiators. However, there are few reports on the use of alkyl-functional ACSi in the treatment of NFs for thermoplastic

polymeric matrices, probably due to their lower reactivity towards hydrolysis [30–34]. It is worth mentioning that there are only a few reports showing compelling evidence of surface-grafted fibers with a high content of ACSi [31,32,35,36].

The synergistic effect of alkaline treatment and ACSi treatment has also been reported [37–40]. It has been observed that alkaline treatment can remove components of low thermal stability, which hinders the processing of PCs using the melt blending method. It can also increase the surface roughness, benefiting the interfacial interaction with hydrophilic polymeric matrices and promoting greater exposure of hydroxyl groups, making them available for subsequent ACSi grafting reactions. On the other hand, treatment with bifunctional ACSi allows one type of functional group of ACSi to react with the surface of NFs, while the other functional group can react or interact with the polymeric matrix [40–43]. The consistent improvement in the properties of NF-polymer composites is intricately linked to the chemical compatibility between these constituents. The enhancement of this compatibility through optimized treatment and functionalization processes results in increased surface adhesion and improved fiber dispersion. These effects culminate in reduced moisture permeability, enhanced absorption of mechanical stresses, and a decrease in fracture propagation, ultimately holding the potential for long-term performance enhancements in such composites.

This research focused on optimizing the conditioning and functionalization of FIx through chemical treatments for its potential application as a reinforcing material in polymeric composites. The main objective was to enhance their physicochemical, thermal, and mechanical properties while achieving compatibility with thermoplastic polymeric matrices. For this purpose, key parameters of the alkali-silane treatment were studied to increase the level of functionalization of FIx. To the best of our knowledge, the effect of the alkali-silane treatment on *Agave lechuguilla* fibers for their utilization as a reinforcement material in PC has not been previously reported. The novelty of this study lies in the comprehensive exploration of the alkali-silane treatment on *Agave lechuguilla* fibers. Hence, this research represents a significant contribution in the field of natural fiber-reinforced polymeric composites. The results of this investigation hold promise for the development of novel applications in industries such as automotive, construction, and packaging, where the demand for sustainable and efficient materials is steadily increasing.

2. Materials and Methods

2.1. Materials

The ixtle fibers (FIx) were obtained from independent traders in the Toluca Valley, State of Mexico. The FIx´s were cut to dimensions of 5 cm for chemical treatments and DMA analysis. High-purity glacial acetic acid (MEYER, Mexico, 99.7% purity) and distilled water (Karal, Mexico, 99.99% purity) were used. In addition, sodium hydroxide (Sigma-Aldrich, Saint Louis, MO, USA, 97% purity), propyltrimethoxysilane or PTMS (Sigma-Aldrich, Saint Louis, MO, USA, 97% purity), hexadecyltrimethoxysilane or HDMS (Sigma-Aldrich, Saint Louis, MO, USA, 85% purity), and (3-aminopropyl)triethoxysilane or APTES (Sigma-Aldrich, Saint Louis, MO, USA, 98% purity) were used.

2.2. Characterization of Ixtle Fiber (FIx)

To determine the thermal stability of FIx, thermogravimetric analysis (TGA) was performed using a TA Instruments Q50 TGA system. The analysis procedure involved placing approximately 20 mg of the sample in a platinum pan and heating it from 25 °C to 600 °C at a heating rate of 10 °C/min under an N2 atmosphere.

Surface morphology observation of FIx was performed through scanning electron microscopy (SEM) using a JEOL JSM-IT100 microscope equipped with a Bruker Flash 6/30 energy-dispersive spectroscopy (EDS) system. The microscope was operated at 17 kV with a backscattered electrons (BEs) detector and a working distance of 15 mm (WD). The microscope was operated at a low vacuum (60 Pa), so the fibers could be observed without

requiring any additional treatment. Micrographs were taken at 200× and 300× magnification and were manually edited, including the scale bar, for better appreciation [5].

Tensile strength properties obtained from tests on DMA equipment are sensitive to the diameter value supplied, so diameter measurement is important. For this purpose, diameter measurements of treated fibers at different alkaline treatment conditions were performed on a Carl Zeiss AXIO ZOOM v16 stereomicroscope. A PlanNeoFluar Z 1.0×/0.25 FWD 56 mm objective with LED illumination was used. Image acquisition was performed with an AxioCam 503 color camera at 50× magnification. Three FIx diameter measurements were performed employing AxioVision software, applying the calibration corresponding to the 50× magnification. A representative image (Figure S1) of the FIx measurements is presented in the Supplementary Material document.

Dynamic mechanical analysis (DMA) in the tension force mode was performed on fibers of 5 cm length with a clamp distance of 10 mm. A TA Instruments Q800 DMA system was used, operated in tension mode with controlled deformation. A force sweep was applied, with one end of the fiber fixed and the other end subjected to a constant deformation rate of 2% per minute. Stress-strain curves were obtained, enabling the determination of maximum stress at rupture, Young's modulus, and percentage of deformation. Additionally, the work in tension (Wb) was calculated by integrating the area under the stress vs. strain curve generated for each specimen, according to the methodology reported by Yan et al. [44].

To assess the effect of the alkaline treatment on the cellulose crystallinity index of FIx, the samples were pulverized using an Ultra ZM 200 centrifugal mill from Retsch and analyzed using a Rigaku Smartlab X-ray diffractometer. The scans were performed in the 2θ range from 5 to 60° at a scanning rate of 10°/min, with a step size of 0.01°, using CuKα radiation (λ = 1.54 angstroms).

The functional groups present on the surface of the fibers before and after the chemical treatments were identified by infrared spectroscopy using an infrared-attenuated total reflectance (IR-ATR) Agilent 4500 Series spectrometer. The samples were analyzed within a spectral range of wavenumbers from 4000 to 700 cm^{-1} with a resolution of 4 cm^{-1}. After the chemical treatments, the samples were dried at 80 °C in an oven with ventilation for eight hours. A single fiber was taken and placed on the diamond tip. To ensure good contact, the clamping device of the equipment was used, which has the function of pressing the sample. The pressure exerted was adjusted until a good resolution of the spectrum was obtained.

2.3. Pretreatment of FIx

Before chemical treatments, dirt and impurities were removed by washing the FIx with water in a 2-L glass reactor. A solution volume to FIx weight ratio of 1:40 was employed. The FIx was agitated at a temperature of 70 °C for 1 h, then filtered and subsequently dried in a vented oven at 80 °C for 8 h. In order to remove waxes and oil from the fibers, the method reported by Vieira was used as a basis [45]. In a glass reactor, the FIx was immersed in 2 L of a 1:2 methanol/toluene solution, utilizing a solution volume to FIx weight ratio of 1:40. The FIx was agitated at a temperature of 70 °C for 1 h. Finally, the FIx was filtered, washed with water, and ultimately dried in a vented oven at 80 °C for 8 h.

2.4. Chemical Modification of FIx

2.4.1. Alkaline Treatment

Treatment conditions were chosen based on several reports relating to the alkaline treatment of natural fibers. Experimental conditions that exhibit promising efficacy in the removal of thermally unstable components and in enhancing the surface exposure of OH groups were favored [46–49]. The FIx was immersed in a NaOH solution (solution volume to FIx weight ratio of 1:40) at different concentrations (2, 5, 8, and 10 wt/vol%) and different temperatures (25 °C and 65 °C) for 1 h. Then the FIx was removed from the solution and

washed with a 5% v/v acetic acid solution several times until adjusted to a neutral pH. Finally, the FIx was dried in a vented oven at 80 °C for 8 h.

2.4.2. Treatment with ACSi

The treatment conditions with the different ACSi were established considering works related to the study of the effect of the amount of water and pH in the reaction medium on the hydrolysis reaction rate of ACSi [50,51]. Studies on the effect of ACSi concentration on the promotion of the grafting reaction in natural fibers were also considered [30,31,52–54]. The ACSi (2, 5, and 8% by weight relative to the fiber weight) were activated through a hydrolysis reaction in a methanol/deionized water solution (6/4 and 8/2); the pH was adjusted using acetic acid (pH = 3 and 5), and they were stirred for 60 min at a temperature of 25 °C. Subsequently, the fibers were immersed in the mixture using a solution volume to FIx weight ratio of 1:25. They were maintained at 25 °C for 1 h. Following this, the fibers were retrieved from the solution and air-dried in an extraction hood at room temperature, then cured for an hour at 120 °C in a ventilated oven. Finally, the fibers were washed twice with methanol to remove residual ACSi and dried at 80 °C for 8 h in a ventilated oven.

3. Results and Discussion

3.1. Alkaline Treatment of FIx

3.1.1. Morphology Analysis

The surface morphology of untreated FIx was examined using scanning electron microscopy (SEM). Figure 1a,b present micrographs of the longitudinal and cross-sectional views of FIx, respectively. Figure 1a reveals a longitudinal arrangement of numerous densely packed microfibrils, along with surface adherences typically associated with waxes and particles that have been previously reported as potential minerals [8,11,13,17,29,55,56]. In the context of this study, the SEM analysis was primarily directed towards examining the impact of washing and alkaline treatment on the cleanliness and surface alterations of the FIX. Another important objective was quantifying the silicon content to validate the effectiveness of silane functionalization. Therefore, only one cross-sectional image is included here to exemplify the fibrillar structure of the FIx.
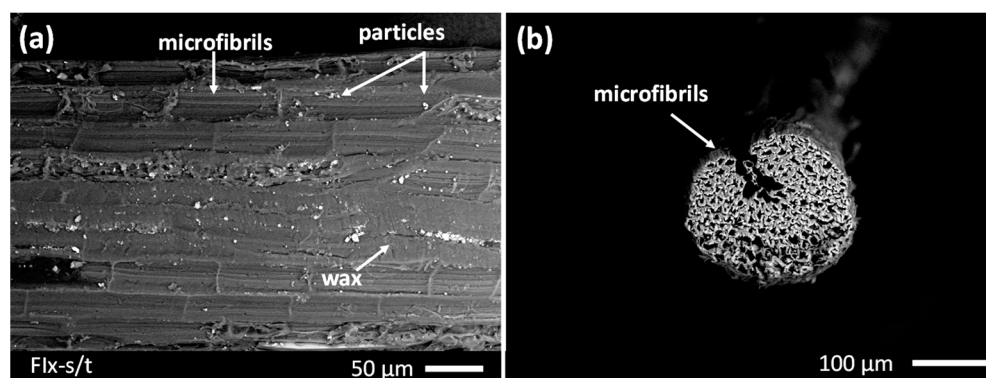

Figure 1. SEM micrograph of untreated Fix: (**a**) longitudinal section; and (**b**) cross section.

Figure 2 displays SEM micrographs of FIx treated at 25 °C with different concentrations of NaOH, which exhibited surface alterations due to alkaline treatment. The quantity of waxes and impurities on the surface of FIx decreased with the increase in the employed NaOH concentration during treatment.

Figure 3 presents SEM micrographs of FIx treated at 65 °C with varying concentrations of NaOH, revealing a cleaner surface and notably enhanced surface roughness compared to untreated FIx and FIx treated at 25 °C. This behavior is attributed to the more severe removal of waxes, hemicellulose, and lignin.

The increase in roughness is anticipated to confer a beneficial effect on enhancing the interfacial adhesion between FIx and the polymeric matrix, as has been reported in other

studies [28,29,57–59]. Notably, in the FIx-6 sample treated with 5% NaOH, the onset of fibrillation was observed.
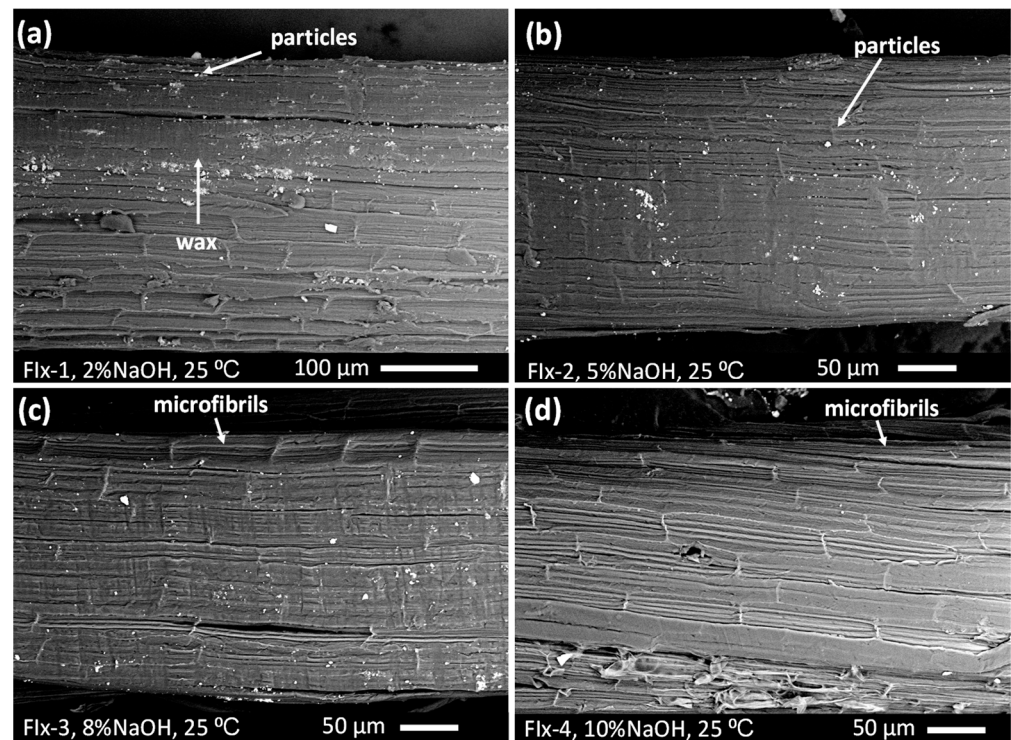

Figure 2. SEM micrograph of FIx samples treated at 25 °C: (**a**) FIx-1, 2% NaOH; (**b**) FIx-2, 5% NaOH; (**c**) FIx-3, 8% NaOH; and (**d**) FIx-4, 10% NaOH.
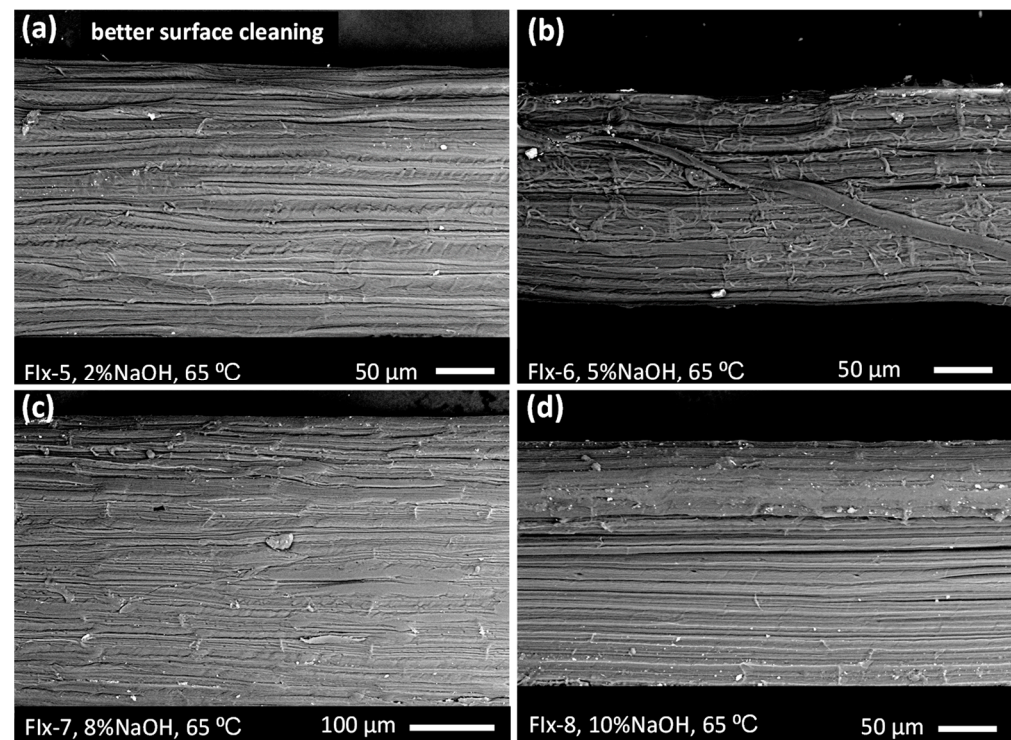
Figure 3. SEM micrograph of FIx samples treated at 65 °C: (**a**) FIx-5, 2% NaOH; (**b**) FIx-6, 5% NaOH; (**c**) FIx-7, 8% NaOH; and (**d**) FIx-8, 10% NaOH.

3.1.2. Thermogravimetric Analysis

The thermal stability of treated and untreated fibers was investigated through thermogravimetric analysis. TGA curves and their derivatives (DTGA) were plotted against temperature. Figure 4a,b depict, respectively, the TGA graphs and DTGA curves of FIx treated at 25 °C with varying NaOH concentrations. In general, it was observed that between 25 °C and 125 °C, all fibers experience a slight weight loss attributed to wax and moisture removal. As the NaOH concentration used in the alkaline treatment increases, a reduction in the moisture content of the treated FIx is evident. This distinction becomes clearer in the DTGA curves, which exhibit a decrease in hemicellulose content—an element of the fiber that absorbs most of the moisture. Notably, the moisture content is linked to capillary water, making complete elimination challenging due to its hydrophilic nature [17,60,61]. Within the range of 200 °C to 317 °C, a weight loss occurs corresponding to hemicellulose decomposition (which, being amorphous, exhibits lower thermal stability than cellulose). This is more distinctly evident in the DTGA curve. Subsequently, the weight loss between 317 °C and 390 °C would correspond to cellulose decomposition. On the other hand, lignin decomposition has been reported to occur within the range of 400 °C to 500 °C [33]. The residue corresponding to 17% by weight at a temperature of 600 °C is attributed to the presence of minerals (Ca, K, Si, Mg, Al, S, and Fe, among others) [15,62–64].
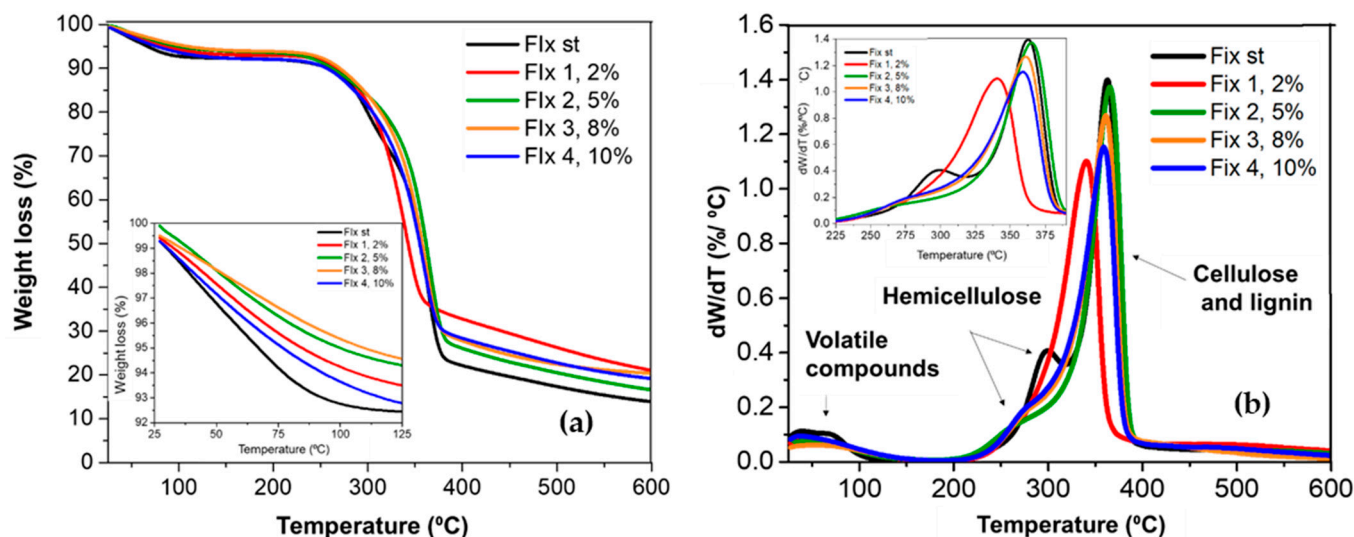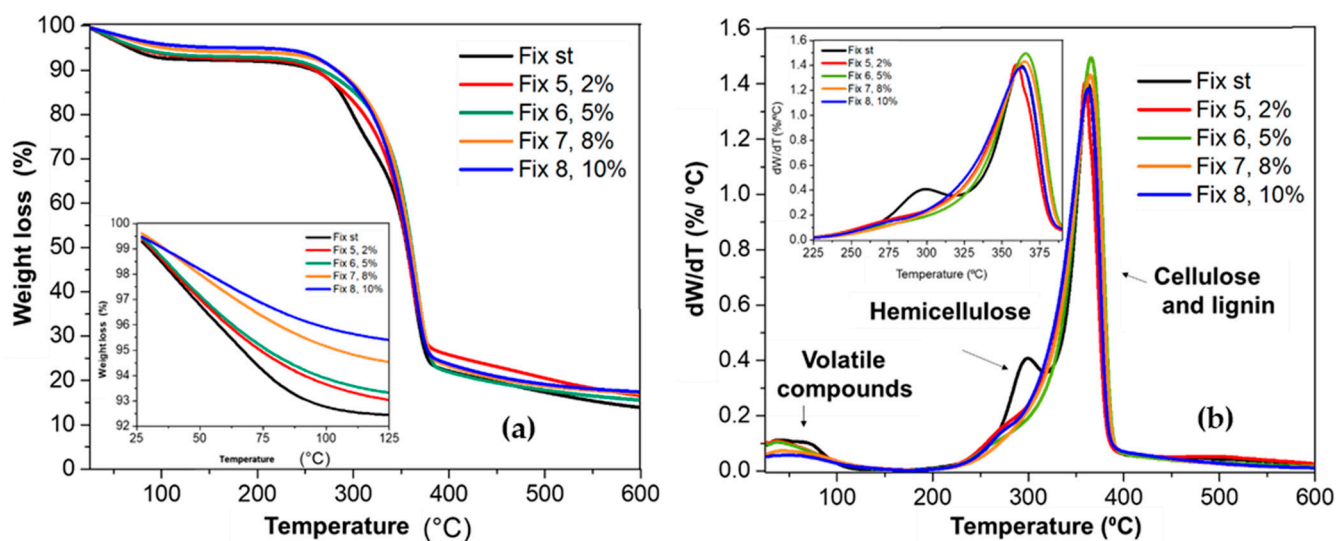

Figure 4. TGA (**a**) and DTGA (**b**) plots as a function of temperature of FIx treated at 25 °C with different NaOH concentrations.

Figure 5a,b, respectively, illustrate the TGA and DTGA graphs of FIx treated at 65 °C with varying NaOH concentrations. A trend towards lower moisture and hemicellulose content is discernible with the increase in NaOH concentration. In fact, in the fiber treated with 8% NaOH, the hemicellulose peak is nearly absent, possibly indicating near-complete removal of hemicellulose from the fiber [17]. In the temperature range around 400 °C, a convolution of different degradation mechanisms is observed, complicating the estimation of cellulose and lignin content through this type of analysis [65]. Nevertheless, TGA analysis provides insights into conditions of alkaline treatment conducive to the removal of significant amounts of moisture, waxes, and hemicellulose—components of lower thermal stability that can hinder the processing of composites with such fibers via melt blending. Additionally, this analysis enables us to define potential formulations for PC, as these fibers could be employed with various polymeric matrices processed within the temperature range of 160 °C to 250 °C, such as LLDPE, PP, PBT, and PA6, among others.

The literature indicates that cellulose content in NFs impacts its mechanical properties, whereas hemicellulose relates to biodegradability and lignin contributes to thermal stability.

References in the literature indicate that the FIx composition consists of 46–48% cellulose, 17–20% hemicellulose, and 11–12% lignin [19,66].

Figure 5. TGA (**a**) and DTGA (**b**) plots as a function of temperature of FIx treated at 65 °C with different NaOH concentrations.

Table 1 presents the results of thermal stability parameters obtained through TGA. The temperatures at which a 5% (T5%), 10% (T10%), and 50% (T50%) mass loss occurs, along with the peak maximum of the DTGA curves (Tmax), are reported. In general, it was observed that subjecting FIx to alkaline treatment results in an increase in the T5% value that can be associated with the elimination of low thermal stability compounds. Nevertheless, a clear correlation with NaOH concentration was not evident.

Table 1. Thermal performance of FIx treated at 25 °C and 65 °C.

| Sample	Temp (°C)	NaOH (%)	T5% [a] (°C)	T10% [a] (°C)	T50% [a] (°C)	Tmax [b] (°C)
FIx s/t (w/o treatment)	25	0	72.2	273.3	358.4	364.5
FIx-1	25	2	122.6	269.1	342.7	343.5
FIx-2	25	5	99.16	261.4	361.5	365.5
FIx-3	25	8	108.6	269.6	357.5	361.5
FIx-4	25	10	76.3	255.4	354.8	359.6
FIx-5	65	2	73.4	259.3	356.6	359.7
FIx-6	65	5	76.2	266.3	360.9	366.1
FIx-7	65	8	233.5	291.9	360.4	365.7
FIx-8	65	10	188.5	281.4	357.4	363.3

[a] Temperatures obtained by TGA at a specific weight loss percentage. [b] Temperature obtained at the maximum of the DTGA curve.

Furthermore, concerning T10%, a reduction in values was observed in all samples treated at 25 °C, but for fibers treated at 65 °C, this reduction in T10% was only evident with lower NaOH concentrations. This reduction in the parameter is likely due to the loss of materials with higher thermal stability, such as hemicellulose and lignin. However, it is noteworthy that in the case of fibers treated at 65 °C with higher NaOH concentrations, an increase in T10% is observed, suggesting that these treatment conditions enhance the thermal stability of the fibers. To draw more robust conclusions regarding this behavior, further investigation through additional studies is warranted.

As for T50% and Tmax, no significant changes were observed due to the treatment, likely because at these temperatures, the degradation processes are not influenced by the changes induced by alkaline treatments.

3.1.3. Dynamic-Mechanical Analysis

The tensile strength properties of NFs are influenced by their geometry, diameter, cellulose content, and crystallinity index. To determine the mechanical properties of FIx, dynamic-mechanical analysis (DMA) in tension mode was chosen, a technique frequently used with polymeric fibers. To our knowledge, the use of DMA to estimate the tensile strength properties of NFs has been reported in only a few studies. Through this analysis, stress-strain curves were obtained, demonstrating a typical behavior following Hooke's Law and similar to those reported for other NFs using a universal testing machine [6,17,67]. In general, across all samples, it was observed that an increase in applied stress leads to reaching a maximum deformation point where the fibers broke. As an example, Figure 6 presents stress-strain curves of FIx samples treated at 25 °C and 65 °C with varying NaOH concentrations. The calculation of Young's modulus was determined at the beginning of the elastic region. On the other hand, rupture strength and deformation were evaluated in the plastic region. Overall, a positive effect of increasing NaOH concentration on FIx tensile strength was observed, and the best result was obtained with the FIx modified with 5% NaOH at 65 °C.
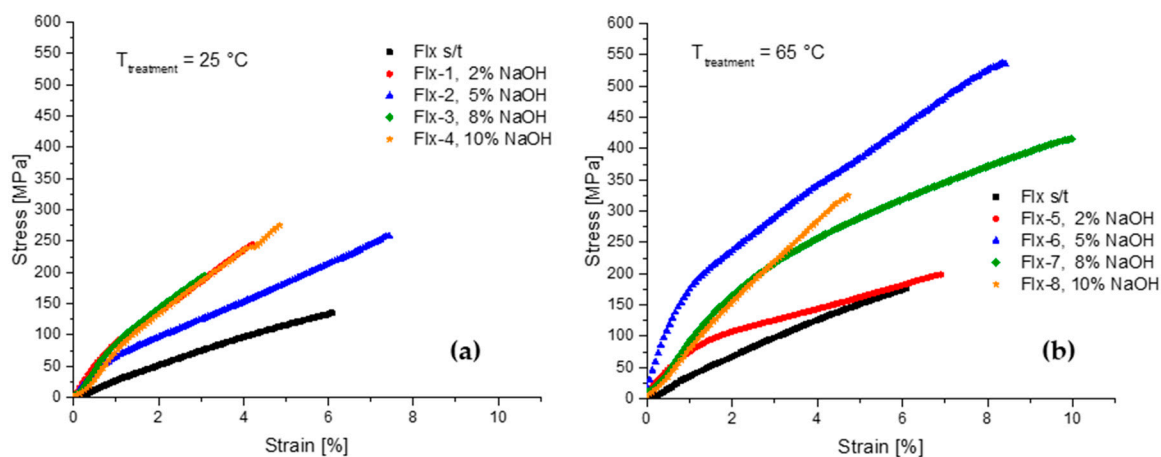
Figure 6. Stress-strain plots obtained by DMA in the stress mode of FIx treated with different NaOH concentrations at (**a**) 25 °C and (**b**) 65 °C.

The tensile properties (tensile strength, % deformation at breakage, and Young's modulus) of FIx treated at 25 °C and 65 °C are summarized in Table 2. It is evident that an increase in NaOH concentration enhances or at least preserves the tensile strength of the FIx. Furthermore, an increase in the percentage deformation at break was observed, as well as an increase in Young's moduli, compared to untreated fibers. It was observed that fibers treated at 65 °C exhibited higher tensile properties compared to the FIx treated at 25 °C. This behavior can be attributed to an increase in temperature and NaOH concentration, which allows for the removal of a greater amount of hemicellulose and lignin, inducing structural changes in the fibers. This modification enables enhanced interaction among cellulose microfibrils through hydrogen bonding. Consequently, when these structurally modified fibers are subjected to tension, a better stress distribution among microfibrils occurs, resulting in increased tensile strength, stiffness, and deformation capacity prior to rupture [28,29]. With respect to the work in tension (Wb), it can be observed in Table 2 that the effect of the alkaline treatment increases the energy required to deform the fiber in tension mode. The improvement in performance with the alkaline treatment conditions at 5% NaOH and 65 °C is almost 5 times the value of the reference FIx, so the improvement in mechanical properties through the alkaline treatment is remarkable.

From the results obtained, it was observed that the alkaline treatment performed at 5% NaOH concentration and 65 °C generated the FIx with better tensile properties (tensile strength and Young's modulus) with respect to the other experiments. However,

in general, all FIx exhibit good tensile properties and are comparable to those of other reported NFs [14].

Table 2. Average mechanical properties of FIx treated at 25 °C and 65 °C.

Sample	Temp. (°C)	NaOH (%)	Tensile Strength [a] (MPa)	Young's Modulus [a] (GPa)	Strain at Breakage [a] (%)	Wb [b] (MJ m^{-3})
FIx s/t (w/o treatment)	-	0	242.33 ± 9.40	7.38 ± 2.56	4.90 ± 0.57	386.4 ± 57.9
FIx-1	25	2	355.53 ± 28.57	7.77 ± 0.22	5.19 ± 0.21	1143.5 ± 184.8
FIx-2	25	5	194.43 ± 11.67	7.40 ± 0.79	5.13 ± 0.14	468.4 ± 170.3
FIx-3	25	8	289.15 ± 30.19	8.86 ± 1.32	8.78 ± 1.66	1532.4 ± 92.2
FIx-4	25	10	293.83 ± 54.59	9.64 ± 1.05	11.82 ± 3.87	1923.4 ± 332.4
FIx-5	65	2	347.73 ± 51.97	10.00 ± 1.42	6.81 ± 0.13	881.8 ± 160.7
FIx-6	65	5	524.25 ± 18.60	14.41 ± 5.06	7.27 ± 1.42	2107.1 ± 557.9
FIx-7	65	8	365.50 ± 12.59	10.21 ± 0.49	8.48 ± 0.67	1879.6 ± 455.7
FIx-8	65	10	329.97 ± 24.68	11.88 ± 1.68	5.56 ± 0.78	1614.6 ± 132.4

[a] Parameters obtained by DMA in tensile mode by triplicate. [b] Work of tension was calculated by integrating the area under the stress-strain curves.

Concluding on the effect of NaOH concentration on the tensile mechanical properties, in experiments conducted at various temperatures, it is evident that there exists an optimal concentration to achieve enhanced tensile strength in fibers. Similar behaviors have been observed by some authors and are attributed to the fact that in untreated fibers, hemicellulose and lignin remain dispersed within the interfibrillar regions, separating cellulose chains from each other, with the cellulose chains existing in a state of tension. When hemicellulose and lignin are partially removed, the tension is released, and fibrils exhibit a greater capacity to reorganize in a more compact manner, thereby promoting higher tensile strength in the fiber. Conversely, if the concentration of the alkaline solution exceeds the optimum, excessive lignin removal may occur, leading to fiber damage and a subsequent reduction in tensile strength properties [68,69]. Therefore, various studies have focused on determining the optimal NaOH concentration for each type of natural fiber, as is the case in the present study.

Regarding the effect of reaction temperature, it is generally observed that higher temperatures during the alkaline treatment result in elevated tensile properties of the FIx. Under ambient reaction conditions, hemicellulose and lignin exhibit greater stability. However, when the temperature is raised to 65 °C, these components with lower thermal stability can be effectively removed by the alkaline solution. The removal of more lignin and hemicellulose between adjacent cellulose chains reduces the distance between the chains, facilitating interactions through hydrogen bonding and thereby promoting enhanced tensile strength in the fiber [28].

3.1.4. X-ray Powder Diffraction Analysis (XRD)

The X-ray diffraction patterns obtained from FIx treated with NaOH at 25 °C and 65 °C are shown in Figure 7a,b, respectively. In the graphs, two main peaks can be observed, which are characteristic of cellulose I. The first peak is broad and has multiplicity at 2θ = 14.88° and 2θ = 16.09°, corresponding to the crystallographic planes (101) and (101), respectively. The second peak is sharp and intense at 2θ = 22.86°, corresponding to the crystallographic plane (002). Additionally, a smaller peak is observed at 2θ = 35°, corresponding to the (040) plane [48,70,71].

In the X-ray diffraction patterns of FIx, no polymorphic transformation is observed due to the different conditions employed in the alkaline treatment. However, changes in the intensity of the main peaks are noticeable. The low-angle, low-intensity peak (16°) represented as I_{am}, and the other higher-intensity peak (23°) represented as I_{002} in Equation (1) correspond to the amorphous and crystalline components of cellulose, respectively. This equation was utilized to measure the crystallinity index (*CI*) of the treated FIx [48,70,71].

$$CI\ (\%) = \frac{I_{002} - I_{am}}{I_{002}} \times 100 \tag{1}$$
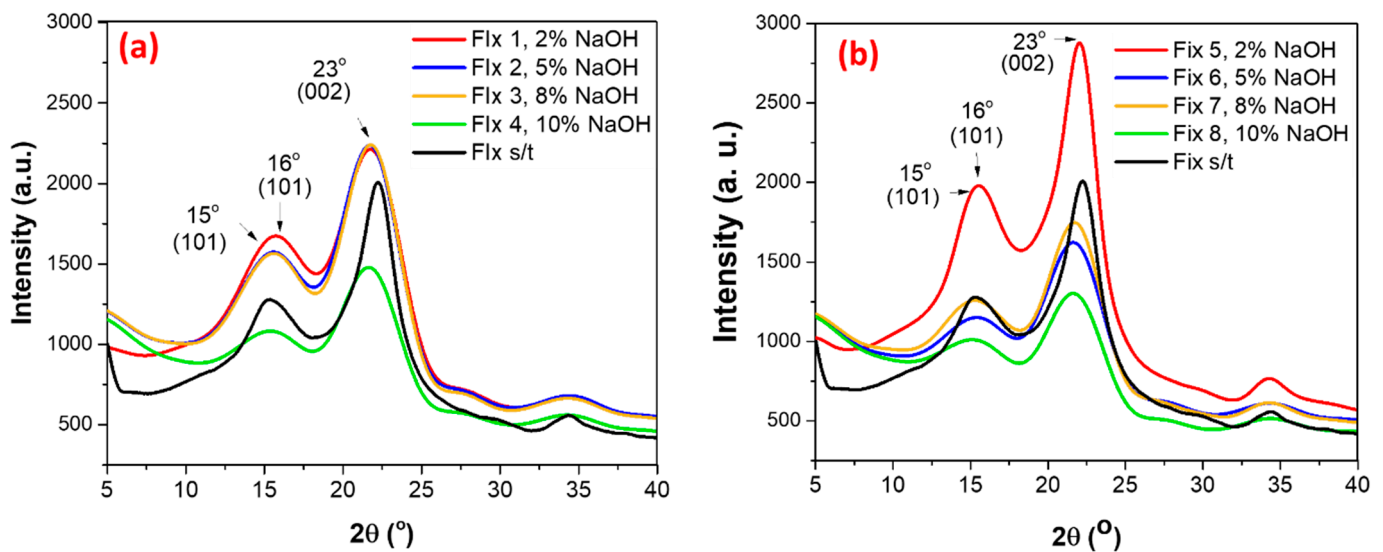
Figure 7. Diffraction patterns of FIx treated at 25 °C (**a**) and 65 °C (**b**).

Table 3 shows the crystallinity index (CI) of FIx treated at 25 °C and 65 °C. In both cases, a trend of an increase in CI with increasing NaOH concentrations can be observed. However, the treatment performed at 65 °C generates fibers with a higher CI, which is attributed to a higher removal of amorphous components (hemicellulose and lignin).

Table 3. Crystallinity index (CI) of FIx treated at 25 °C and 65 °C.

| NaOH (%) | T = 25 °C | | T = 65 °C | |
	Sample	CI [a] (%)	Sample	CI [a] (%)
0	FIx s/t	67.4	-	-
2	FIx-1	63.1	FIx-5	62.2
5	FIx-2	73.4	FIx-6	76.9
8	FIx-3	66.9	FIx-7	74.0
10	FIx-4	80.5	FIx-8	78.2

[a] Calculated from XRD data using Equation (1).

As the concentration of the alkaline solution increases, a portion of lignin and hemicellulose in the amorphous region begins to be removed. Under these conditions, reordering of the amorphous region of cellulose can occur, transforming it into crystalline regions. In our study, we observed that starting from a concentration of 5% NaOH (at different temperatures), there is an increase in the crystallinity index (in the range of 8 to 19% at 25 °C and 10 to 16% at 65 °C). This increase can be attributed to the conversion of a fraction of amorphous regions into crystalline ones. Similar results regarding the effect of alkaline solution concentration on the treatment of natural fibers and its impact on crystallinity index have been reported in the literature [28,68,69].

Based on our results, we consider that the stiffness of natural fibers is a function of the content of crystalline regions within cellulose microfibrils, as well as the content of other components such as lignin, which serves as a binding material and holds the cellulose microfibrils together. In other words, a higher concentration of NaOH may promote an increase in the crystallinity index, potentially enhancing fiber stiffness. However, this effect can be counteracted by a defibrillation process [68,69]. This combination of effects may lead to the absence of a direct correlation between the Young's modulus and the crystallinity index.

3.2. Functionalization of FIx with Silane

The fibers treated with the highest Young's modulus value were obtained through the alkaline treatment carried out with 5% NaOH at 65 °C. Consequently, these reaction conditions were chosen for upscaling and obtaining enough FIx to conduct the optimization study of the ACSi treatment. Three types of ACSi were investigated: trimethoxysilylpropylsilane (PTMS), γ-aminopropyltriethoxysilane (APTES), and hexadecyltrimethoxysilane (HDMS).

As previously described, the grafting reaction mechanism proceeds primarily in two stages. In the first stage, the hydrolysis reaction rate of ACSi is influenced by the amount of water and the pH of the reaction medium. In the second stage, the ACSi grafting reaction on the fiber surface is affected by the ACSi concentration and temperature [72–74]. In our experimental design, we investigated the effect of ACSi concentration in the reaction medium and the methanol/water ratio on the grafting content. pH and temperature were maintained constant, which were selected based on other studies [31].

3.2.1. FTIR Analysis of Non-Functionalized FIx

Figure 8 displays the FTIR spectra of untreated FIx and alkaline-treated FIx. The spectra of these samples exhibit absorption bands typical of lignocellulosic fibers in the fingerprint region (1800 to 800 cm^{-1}). In the spectrum of untreated FIx, a peak at 3332 cm^{-1} is observed, attributed to the stretching vibration of O-H groups. Hydroxyl groups are present in the major components of FIx (cellulose, hemicellulose, and lignin). The peaks at 2919 and 2884 cm^{-1} are assigned to aliphatic C-H stretching (cellulose and hemicellulose) in symmetric and asymmetric vibrational modes, respectively. Vibrations at 1615 cm^{-1} and 1510 cm^{-1} are related to the aromatic rings of lignin. The absorption peak at 1736 cm^{-1} corresponds to the stretching vibration of the C=O bond in carboxyl groups of hemicellulose, but can also be associated with lignin structure. Furthermore, the band at 1235 cm^{-1} results from the C-O stretching vibration of the acetyl group in lignin [10,11,24,28,36,71,75,76]. In the Supplementary Material document, Table S1 presents the FTIR signal assignments for the FIx modified by alkaline treatment.
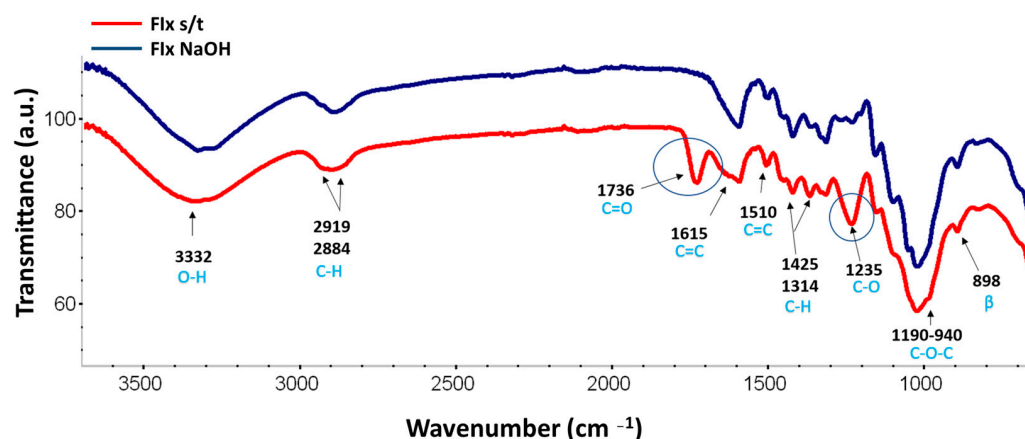
Figure 8. FTIR spectra of FIx without and with alkaline treatment.

In the case of alkaline-treated FIx, the elimination of the absorption peak at 1736 cm^{-1} attributed to C=O bonds of hemicellulose is clearly observed, along with a notable reduction in the 1235 cm^{-1} peak related to lignin C-O groups. This result also suggests that lignin removal occurs during the alkaline treatment process. This analysis is consistent with the TGA results, which indicate that the alkaline treatment effectively removed hemicellulose, lignin, as well as fats or impurities.

3.2.2. Analysis of FIx Functionalized with Silane Coupling Agents (ACSi)

As previously described, hydroxyl groups on the fiber surface can react with hydrolyzed silane coupling agents (Si-OH) and can be grafted onto the fiber surface through

a condensation reaction. On the other hand, they can also undergo self-condensation into polysiloxanes, forming Si-O-C and Si-O-Si bonds. Additionally, during the reaction, ACSi (or polysiloxanes) may be merely adsorbed (not grafted) onto the surface of the FIx, and the presence of unhydrolyzed ACSi can also be shown, which would be identified through Si-OH and Si-OCH$_3$ functional groups, respectively [71,77]. However, in the spectra of fibers treated with ACSi, many of these peaks are scarcely visible due to their overlap with signals from the organic components of the FIx, particularly in the region between 1200 and 900 cm^{-1}.

Analysis of FIx Functionalized with PTMS

Figure 9a displays the FTIR spectra of FIx treated with PTMS using a methanol/water ratio of 8/2. Comparing it with the untreated FIx spectrum, it was observed that only at the 8% ACSi concentration did a decrease in the intensity of the hydroxyl group band occur, which indicates a successful ACSi grafting reaction under these reaction conditions [35,66,67]. The spectrum of this sample also exhibits peaks at 2900 and 2820 cm^{-1}, assigned to the aliphatic C-H bond of PTMS in symmetric and asymmetric vibrational modes, respectively. Subtle indications of silane grafting are discernible in the FTIR spectra of PTMS-modified FIx at a methanol/water ratio of 8/2. This phenomenon can be attributed to the elevated methanol concentration, which tends to decelerate the condensation reaction, thereby promoting grafting. Consequently, a diminishment in OH groups is discerned, yet the signals corresponding to Si-O-C and Si-O-Si groups exhibit relatively subdued intensities, likely attributed to the grafting of ACSi rather than polysiloxane oligomers.

Figure 9b presents the FTIR spectra of FIx treated with PTMS using a methanol/water ratio of 6/4. In the case of FIx treated with 5% and 8% PTMS, signals were observed at 2964 cm^{-1} and 2865 cm^{-1} attributed to C-H bonds, at 780 cm^{-1} assigned to Si-O-Si bonds, and at 1250 cm^{-1} corresponding to Si-O-C bonds of PTMS. This might indicate a prevalence of polisiloxane formation rather than an ACSi grafting reaction. As reported by Peña et al., the use of a higher amount of water in the reaction medium increases the hydrolysis reaction rate, leading to a greater number of silanols and rapid polisiloxane formation [59,60].

Spectra in Figure 9b show more intense signals at 5% in the 780 cm^{-1} and 1259 cm^{-1} bands. This behavior can be explained by a possible grafting of oligomers derived from silane condensation. This is not the case at 8% because increasing the silane concentration promotes condensation over grafting, leading to higher molecular-weight polysiloxanes that can be removed during washing.

Analysis of FIx Functionalized with APTES

Figure 10a exhibits the FTIR spectra of FIx treated with APTES using a methanol/water ratio of 8/2. It can be observed that APTES concentrations of 2%, 5%, and 8% lead to a reduction in the intensity of the hydroxyl band, indicating surface modification of FIx [35,55,67]. Regarding the peaks associated with APTES, some are not discernible due to overlap with signals from the organic components of FIx. This is exemplified in the regions at 3300 cm^{-1} and 3290 cm^{-1}, which correspond to the asymmetric and symmetric stretching modes of NH$_2$, respectively. A similar situation arises with the peak related to the C-N bond in the 1400 cm^{-1} region. On the other hand, observable signals include the vibrations of aliphatic C-H bonds at 2920 cm^{-1} and 2830 cm^{-1}, as well as the peak at 1630 cm^{-1} associated with NH$_2$ bending deformation modes [78–80]. Additional peaks are evident in the region of aliphatic C-H bond vibrations at 2920 cm^{-1} and 2830 cm^{-1}, attributed to APTES. Furthermore, new peaks appear at 1380 cm^{-1} and 960 cm^{-1}, corresponding to symmetric stretching of Si-O-C$_{cellulose}$ bonds, and an additional peak at 780 cm^{-1} is attributed to Si-O-Si bonding [71,77,78]. In the Supplementary Material document, Table S2 presents the FTIR signal assignments for silane-treated FIx.
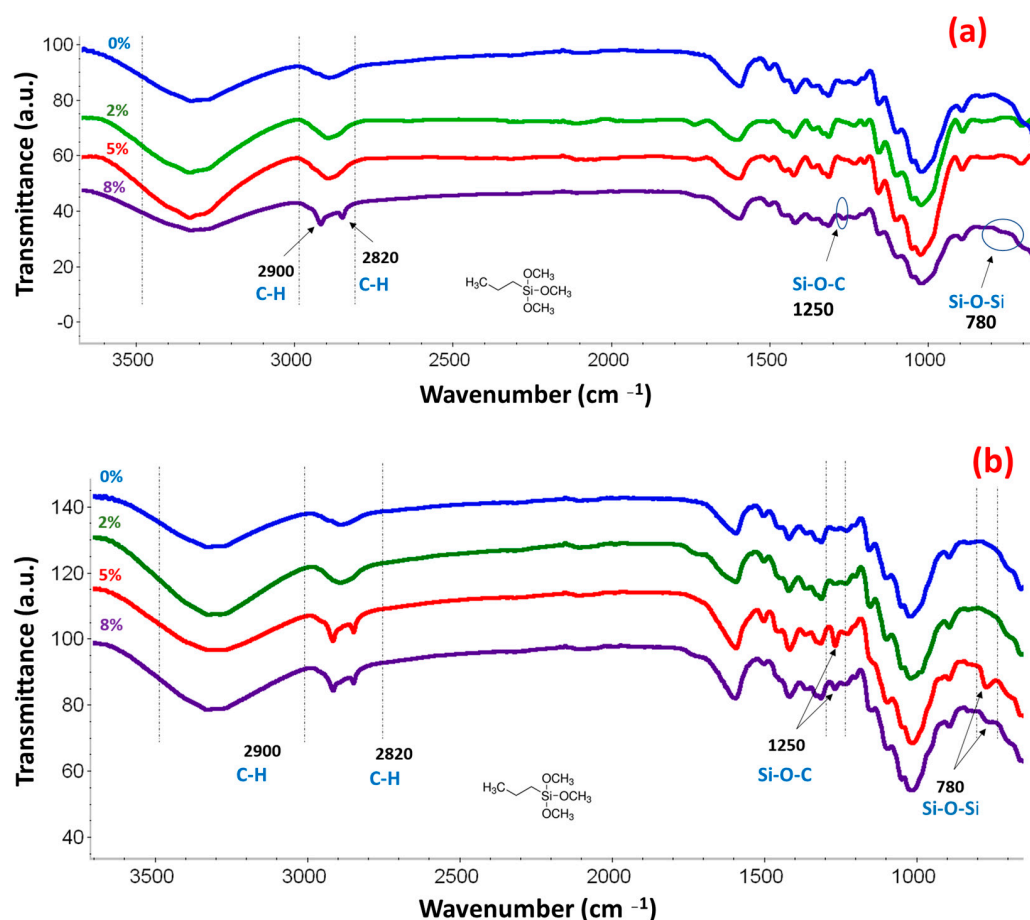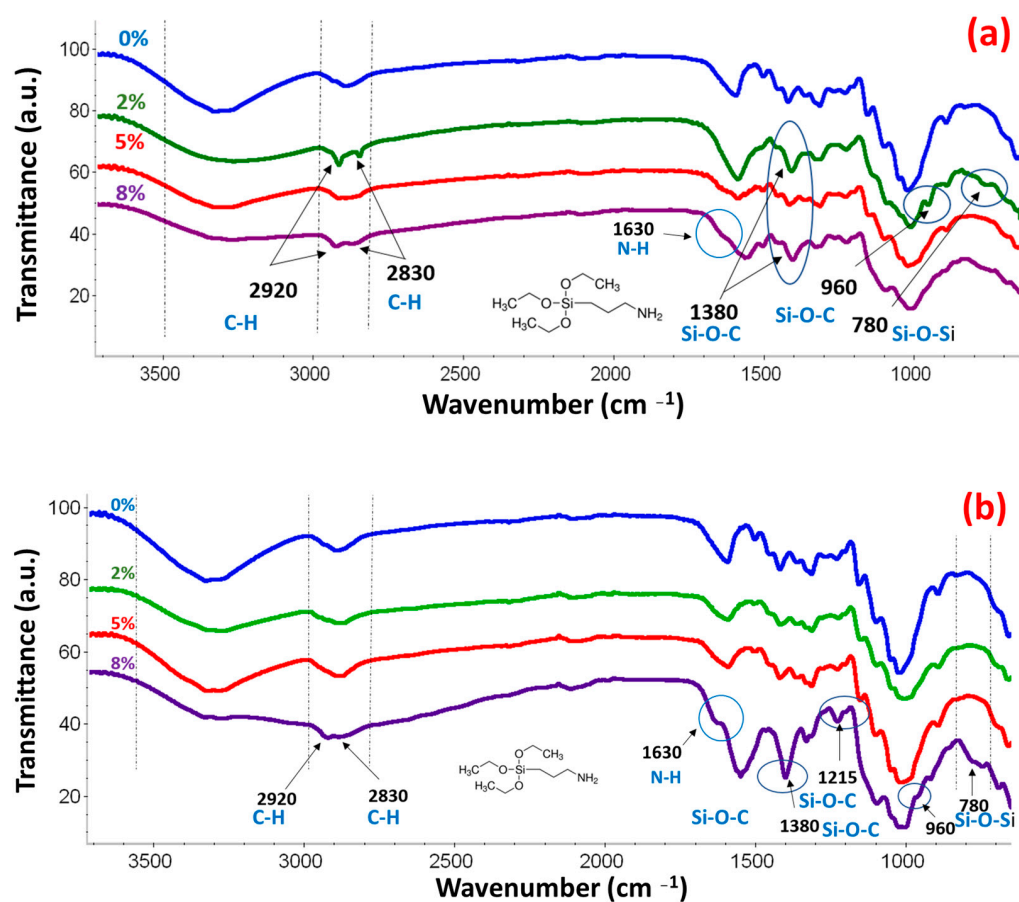
Figure 9. FTIR spectra of PTMS-treated FIx with a methanol/water ratio of 8/2 (**a**) and 6/4 (**b**). 0% PTMS (blue line), 2% PTMS (green line), 5% PTMS (red line), and 8% PTMS (purple line).

In Figure 10b, the FTIR spectra of FIx treated with APTES using a methanol/water ratio of 6/4 are shown. Notably, only at an 8% APTES concentration is a significant reduction in hydroxyl band intensity observed [36,67,77]. Concerning the peaks associated with APTES, vibrational peaks of aliphatic C-H bonds are noticeable at 2920 cm^{-1} and 2830 cm^{-1}. Also, the peak at 1630 cm^{-1} related to NH_2 bending deformation modes is more clearly discernible, and a novel peak at 780 cm^{-1} attributed to the Si-O-Si bond appears [78,80].

Additionally, peaks are evident in the region of aliphatic C-H bond vibrations at 2920 cm^{-1} and 2830 cm^{-1}, as well as an additional peak at 780 cm^{-1} attributed to APTES's Si-O-Si bonding. Furthermore, new peaks at 1380 cm^{-1} and 960 cm^{-1}, attributed to symmetric stretching of Si-O-C$_{cellulose}$ bonds, are evident in this sample, along with an asymmetric stretch of the same bond at 1215 cm^{-1}. Notably, the peak at 1380 cm^{-1} is more intense in this sample compared to the sample obtained with the same 8% APTES concentration but with an 8/2 methanol/water ratio.

The grafting reaction with APTES was favored when a methanol/water ratio of 6/4 was employed. This phenomenon could be linked to the higher degree of dispersion of APTES under these conditions due to its greater polar nature. Furthermore, the grafting reaction, even at low ACSi concentrations, was likely promoted because APTES is more reactive than PTMS and HDMS [72,73,76].

Figure 10. FTIR spectra of APTES-treated FIx with a methanol/water ratio of 8/2 (**a**) and 6/4 (**b**). 0% APTES (blue line), 2% APTES (green line), 5% APTES (red line), and 8% APTES (purple line).

Analysis of FIx Functionalized with HDMS

In Figure 11a,b, the FTIR spectra of FIx treated with HDMS using a methanol/water ratio of 8/2 and 6/4, respectively, are presented. In both cases, there was no significant decrease in the intensity of the hydroxyl group band. This could be attributed to the non-polar nature of HDMS, which might hinder its dispersion in the reaction medium. Nevertheless, in all HDMS-treated FIx samples, peaks at 2900 cm^{-1} and 2820 cm^{-1} are evident, corresponding to the aliphatic C-H bond of HDMS in symmetric and asymmetric vibration modes, respectively. This behavior could indicate the occurrence of grafting reactions, albeit to a lesser extent compared to APTES-functionalized FIx samples.

3.2.3. Elemental Analysis and Chemical Mapping of FIx by SEM–EDS

To confirm the grafting reaction of ACSi on the surface of the FIx, the elemental chemical composition and chemical mapping of elements present in ACSi were determined using the SEM–EDS technique. The analyses were performed in triplicate at different regions of the sample to obtain a representative and descriptive collection of ACSi distribution on the NF surface. The values in Si composition were tracked in the functionalized fibers with different ACSi. These results are summarized in Table 4. It is important to clarify that only fibers that showed a reduction in hydroxyl group band intensity by FTIR were analyzed. The Si percentage was estimated considering only the elements identified in the EDS spectra of each fiber series analyzed. Some representative EDS spectra are presented in Figure 12. As mentioned earlier, the natural FIx composition includes trace amounts of minerals, including Si. Analysis of fibers functionalized with PTMS and HDMS indicate that using a methanol/water ratio of 8/2 yielded a higher content of ACSi grafting compared to a 6/4 ratio. Conversely, in the case of fibers functionalized with APTES, a higher grafting

content was achieved with a 6/4 ratio. This behavior could be attributed to the less polar nature of PTMS and HDMS compared to APTES, influencing their dispersion degree in the reaction medium. The SEM–EDS analysis allowed us to conclude that APTES is the ACSi with which the highest grafting content was achieved.
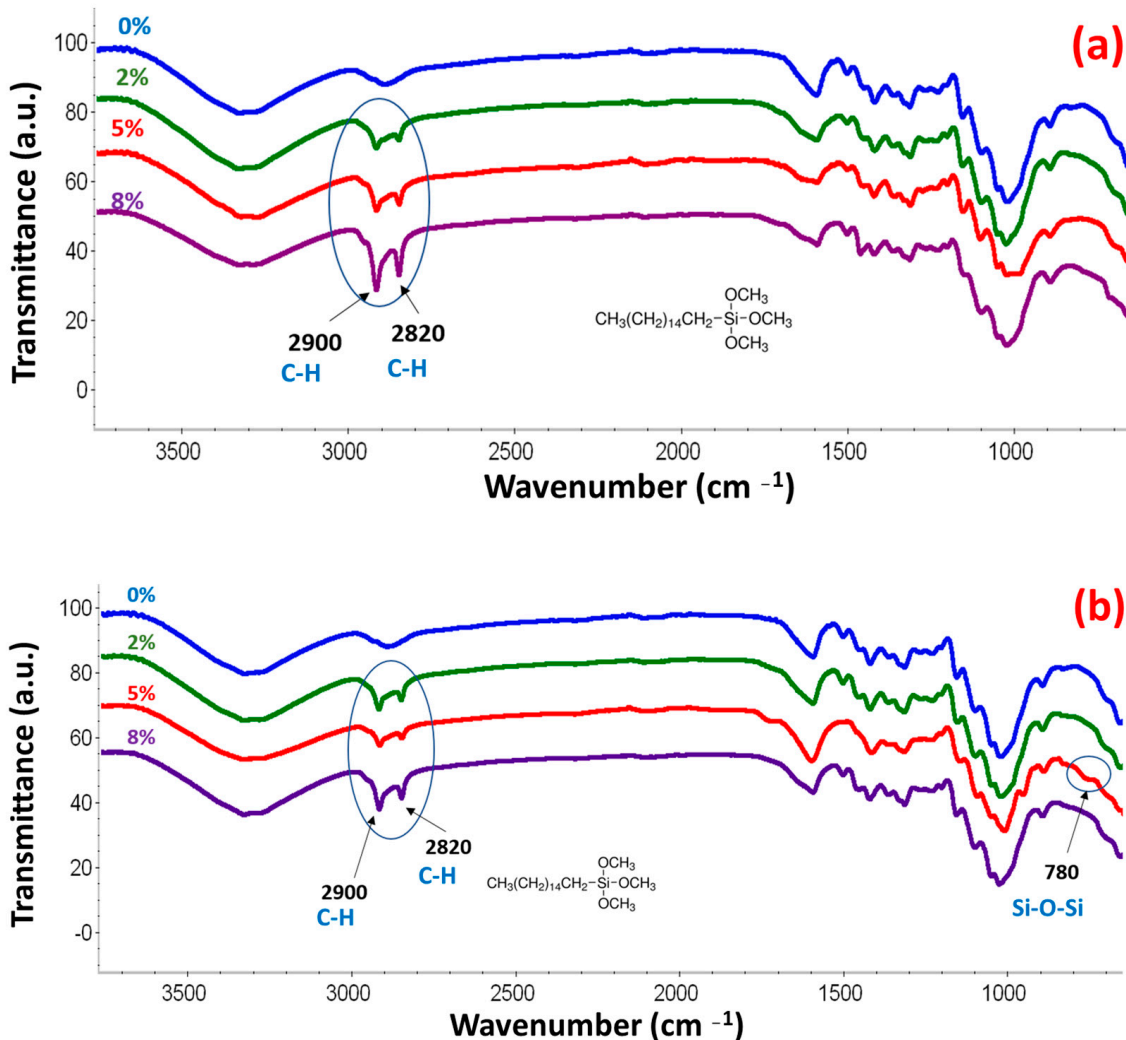

Figure 11. FTIR spectra of HDMS-treated FIx with a methanol/water ratio of 8/2 (**a**) and 6/4 (**b**). 0% HDMS (blue line), 2% HDMS (green line), 5% HDMS (red line), and 8% HDMS (purple line).

Table 4. Si content in functionalized FIx.

Sample	Methanol/Water Ratio	ACSi [%] [a]	Si [%] [b] (Average)
FIx s/t	0	0	0.02
FIx-PTMS	8/2	8	0.84
FIx-PTMS	6/4	5	0.23
FIx-HDMS	8/2	5	0.62
FIx-HDMS	6/4	8	0.33
FIx-APTES	8/2	8	2.12
FIx-APTES	6/4	8	8.20

[a] ACSi dosification percentage during silane treatment. [b] Si percentage estimated as the average of 3 FIx samples analyzed by SEM–EDS considering elements identified in the EDS spectra.
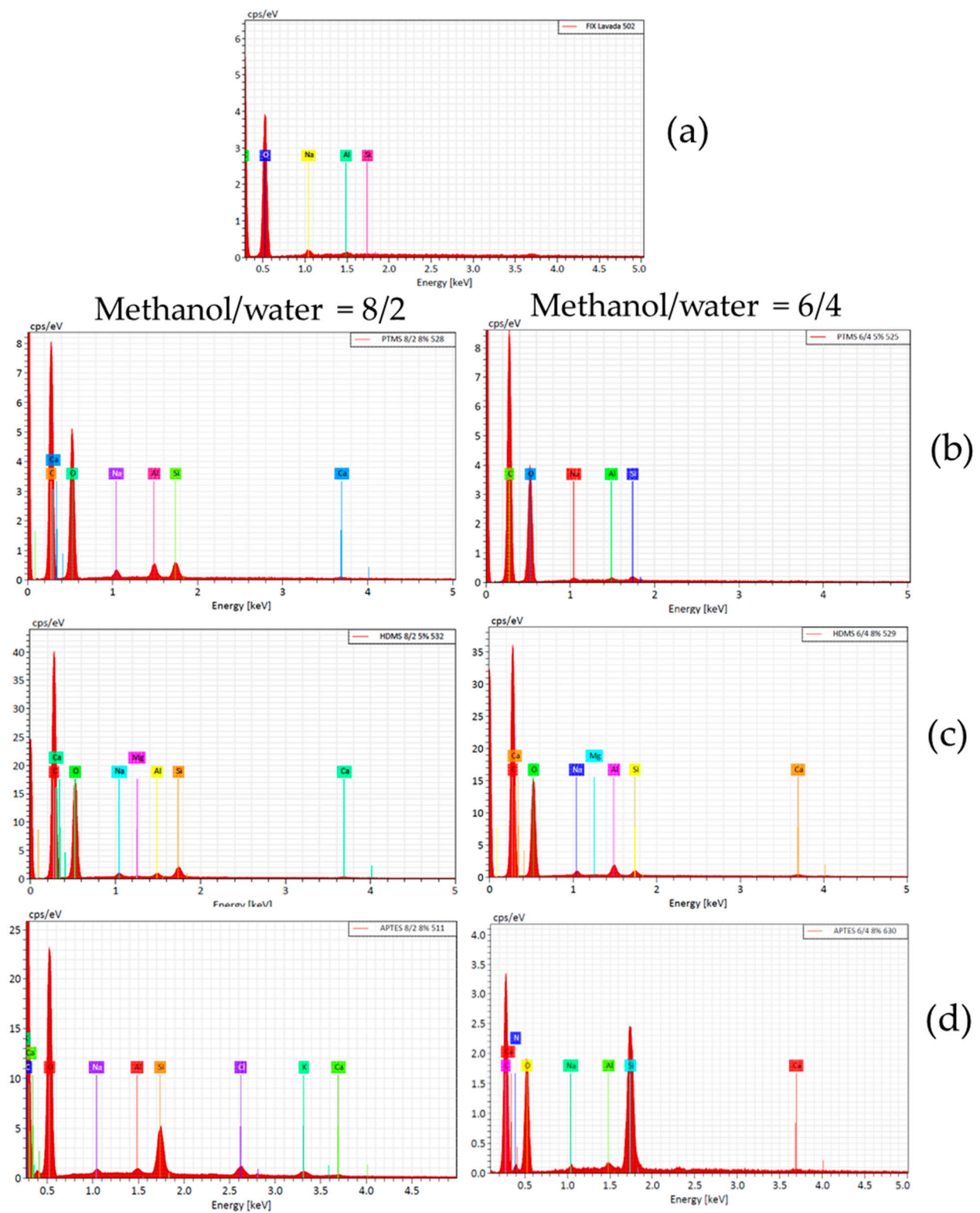
Figure 12. EDS spectra of fibers (**a**) without ACSi and functionalized with different ACSi at methanol/water ratios of 8/2 and 6/4: (**b**) PTMS, (**c**) HDMS, and (**d**) APTES. Spectra belonging to the SEM micrographs in Figure 13, from which the Si element composition was estimated, are provided in Table 4.
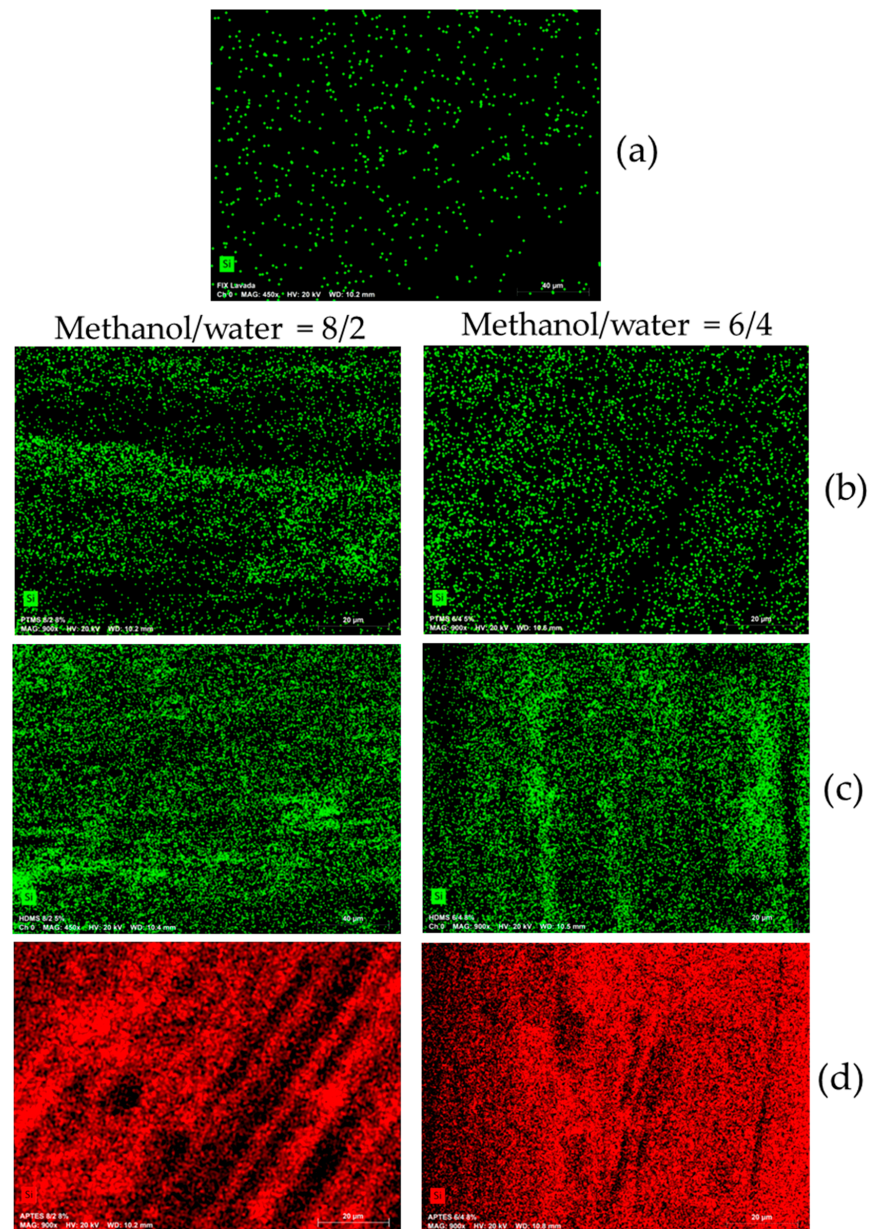
Figure 13. Micrographs (SEM–EDS) with Si mapping on the surface of fibers functionalized with different ACSi with methanol/water ratios of 8/2 and 6/4: (**a**) without ACSi, (**b**) PTMS, (**c**) HDMS, and (**d**) APTES.

In Figure 13, micrographs with elemental analysis obtained by SEM–EDS are displayed, each representing one of the analyzed fiber series. Through this analysis, the dispersion of Si on the fiber surface was observed. In most of the samples, Si dispersion was found to be homogeneous. The fibers functionalized with APTES exhibited the richest Si concentration areas. It is noteworthy that there are few studies on NF functionalization that combine FTIR analysis with SEM–EDS analysis to quantitatively report the grafted Si content on the fiber surface. These works reported a lower Si content on the NF surface compared to what was obtained in our study, thus allowing us to conclude that the ACSi grafting reactions under the functionalization conditions evaluated in this work were highly successful [28,67,68].

4. Conclusions

The combined use of alkaline-silane chemical treatments on ixtle fibers (FIx) enabled the preparation of conditioned fibers for potential application as reinforcement material in polymer composites.

The alkaline treatment removed non-cellulosic components, resulting in fibers with improved thermal stability and higher tensile strength. Additionally, morphological analysis confirmed that employing a temperature of 65 °C led to increased surface cleanliness, which is advantageous for grafting reactions with silane coupling agents (ACSi).

Through FTIR and SEM–EDS analyses, the grafting reaction of different ACSi onto the fiber surface was validated, and the Si content on the fiber surface was quantified. The highest ACSi grafting content in FIx was achieved using APTES with a methanol/water ratio of 6/4 and an 8% APTES concentration. Notably, the obtained grafting content far exceeded that of similar reports.

One of the advantages of FIx over other natural fibers is its length and mechanical strength, which makes optimizing the level of silane functionalization of ixtle fibers to enhance their compatibility in polymer composites highly desirable. Functionalized FIx has the potential to enhance fiber-polymer matrix adhesion, thereby contributing to the development of composite materials with favorable morphological, thermal, and mechanical properties. The proposed surface functionalization strategy for the FIx enables the accurate selection of the most compatible silane type based on the polarity of the polymer matrix. Furthermore, it improves the homogeneity of functional group distribution on the fiber surface, as evidenced by the Si group mapping. This endeavor holds great promise for developing applications of these composites in the automotive and construction sectors.

References

1. Soriano-Corral, F.; Calva-Nava, L.A.; Hernández-Gámez, J.F.; Hernández-Hernández, E.; González-Morones, P.; Ávila-Orta, C.A.; Soria-Arguello, G.; Fonseca-Florido, H.A.; Covarrubias-Gordillo, C.A.; Díaz de León-Gómez, R.E. Influence of Ethylene Plasma Treatment of Agave Fiber on the Cellular Morphology and Compressive Properties of Low-Density Polyethylene/Ethylene Vinyl Acetate Copolymer/Agave Fiber Composite Foams. *Int. J. Polym. Sci.* **2021**, *2021*, 9150310. [CrossRef]

2. Muralidhar, B.A. Characterization of Sisal/Polypropylene Composites Treated with Plasma. *Text. Leather Rev.* **2020**, *3*, 202–212. [CrossRef]
3. Frollini, E.; Bartolucci, N.; Sisti, L.; Celli, A. Poly(butylene succinate) reinforced with different lignocellulosic fibers. *Ind. Crops Prod.* **2013**, *45*, 160–169. [CrossRef]
4. Valea, A.; Corcuera, M.A.; Eceiza, A.; Gonzalez, M.L. Modificación superficial de fibras de sisal para su utilización como refuerzo en materiales composites de matriz polipropileno. *Mater. Compuestos* **2019**, *32*, 69–75.
5. Yan, Y.; Xiao, L.; Teng, Q.; Jiang, Y.; Deng, Q.; Li, X.; Huang, Y. Strong, Tough, and Adhesive Polyampholyte/Natural Fiber Composite Hydrogels. *Polymers* **2022**, *14*, 4984. [CrossRef] [PubMed]
6. Annandarajah, C.; Li, P.; Michel, M.; Chen, Y.; Jamshidi, R.; Kiziltas, A.; Hoch, R.; Grewell, D.; Montazami, R. Study of Agave Fiber-Reinforced Biocomposite Films. *Materials* **2018**, *12*, 99. [CrossRef] [PubMed]
7. Castillo-Quiroz, D.; Berlanga-Reyes, C.; Pineda, A. *Recolección, Extracción y Uso de la Fibra de Lechuguilla (Agave lechuguilla Torr.) en el Estado de Coahuila*; INIFAP-CIRNE: Río Bravo, Mexico, 2005; pp. 1–13.
8. Reyes-Agüero, J.; Aguirre-Rivera, J.; Peña-Valdivia, C. Biology and use of *Agave lechuguilla* Torrey. *Bot. Sci.* **2000**, *67*, 75–88. [CrossRef]
9. Hernández, S.R.; Lugo, E.C.; Díaz, L.; Villanueva, S. Extraction and indirect quantification of saponins from the *Agave lechuguilla* Torrey. *e-Gnosis* **2005**, *3*, 1–9.
10. Cruz, R.A.; Mendotza-Martínez, A.; Heinze, T. Synthesis and characterization of graft copolymers from natural fibers. *Int. J. Polym. Mater. Polym. Biomater.* **2002**, *51*, 661–674. [CrossRef]
11. Carmona, J.E.; Morales-Martínez, T.K.; Mussatto, S.I.; Castillo-Quiroz, D.; Ríos-González, L.J. Propiedades químicas, estructurales y funcionales de la lechuguilla (*Agave lechuguilla* Torr.). *Rev. Mex. Cienc. For.* **2017**, *8*, 100–122. [CrossRef]
12. Infante-Torres, O. El Aprovechamiento de Fibras Naturales del Altiplano Potosino como Materia Prima para el Desarrollo de Productos, a Través de un Modelo de Clasificación. Master's Thesis, Universidad Autónoma de San Luis Potosí, San Luis Potosí, Mexico, 2011.
13. Flores-Dávila, M.P. La Lechuguilla. Un recurso olvidado. Secretaria del Medio Ambiente. *Bordeando Monte* **2018**, *51*, 3–8.
14. Madhu, P.; Sanjay, M.R.; Jawaid, M.; Siengchin, S.; Khan, A.; Pruncu, C.I. A new study on effect of various chemical treatments on *Agave americana* fiber for composite reinforcement: Physico-chemical, thermal, mechanical and morphological properties. *Polym. Test.* **2020**, *85*, 106437. [CrossRef]
15. García Hernández, Z.; Miranda Teran, Z.N.; González-Morones, P.; Yañez-Macías, R.; Rosales, S.G.S.; Yolotzin-Romero, G.; Sifuentes-Nieves, I.; Hernández-Hernández, E. Performance of nylon 6 composites reinforced with modified agave fiber: Structural, morphological, and mechanical features. *J. Appl. Polym. Sci.* **2021**, *138*, 50857. [CrossRef]
16. Moscoso-Sánchez, F.J.; Alvarad, A.; Martínez-Chávez, L.; Hernández-Montelongo, R.; Escamilla, V.V.F.; Escamilla, G.C. The effects of henequen cellulose treated with polyethylene glycol on properties of polylactic acid composites. *BioResources* **2019**, *14*, 2707–2726. [CrossRef]
17. Hidalgo-Reyes, M.; Caballero-Caballero, M.; Hernández-Gómez, L.H.; Urriolagoitia-Calderón, G. Chemical and morphological characterization of Agave angustifolia bagasse fibers. *Bot. Sci.* **2015**, *93*, 807–817. [CrossRef]
18. Caldera-Briseño, C.A.; Miramontes de León, D.; Hernández-Guerrero, A.; Trujillo-Barragán, M. Caracterización de materiales compuestos de matriz polimérica con fibra de ixtle. In Proceedings of the XVIII Congreso Internacional Anual de la SOMIM, Salamanca, Mexico, 19–21 September 2012; pp. 673–682.
19. Torres-Arellano, M.; Renteria-Rodríguez, V.; Franco-Urquiza, E. Mechanical Properties of Natural-Fiber-Reinforced Biobased Epoxy Resins Manufactured by Resin Infusion Process. *Polymers* **2020**, *12*, 2841. [CrossRef] [PubMed]
20. Franco-Urquiza, E.A.; Saleme-Osornio, R.S.; Ramírez-Aguilar, R. Mechanical Properties of Hybrid Carbonized Plant Fibers Reinforced Bio-Based Epoxy Laminates. *Polymers* **2021**, *13*, 3435. [CrossRef]
21. Abhilash, S.S.; Singaravelu, D.L. Effect of Fiber Content on Mechanical, Morphological, and Vibration Damping Characteristics of Natural Fiber-reinforced Composite Fuel Tanks. *J. Nat. Fibers* **2022**, *19*, 14994–15007. [CrossRef]
22. Narendiranath Babu, T.; Rajkumar, E.; George, G.; Jobai, J.; Rama Prabha, D. Tensile and flexural properties of Tampico fibres and E-glass fibre composites reinforced with epoxy resin. *Proc. Inst. Mech. Eng. Part L J. Mater. Des. Appl.* **2021**, *235*, 2783–2796. [CrossRef]
23. Pérez-Pérez, A.; Bello-Silva, E.; Carro-Sánchez, S.; Romero-Mitre, R.D.; Cervantes-Hernández, B.A. Obtaining and Study of Cellulose Microcrystals from Agave Lechugila. *Int. Res. J. Eng. Technol.* **2019**, *6*, 7238–7241.
24. Jamilah, U.L.; Sujito, S. The improvement of ramie fiber properties as composite materials using alkalization treatment: NaOH concentration. *Indones. J. Mater. Sci.* **2021**, *22*, 62. [CrossRef]
25. Sathish Kumar, R.; Muralidharan, N.; Sathyamurthy, R. Optimization of Alkali Treatment Process Parameters for Kenaf Fiber: Experiments Design. *J. Nat. Fibers* **2020**, *19*, 4276–4285. [CrossRef]
26. Mochane, M.J.; Magagula, S.I.; Sefadi, J.S.; Mokhena, T.C. A Review on Green Composites Based on Natural Fiber-Reinforced Polybutylene Succinate (PBS). *Polymers* **2021**, *13*, 1200. [CrossRef]
27. El Oudiani, A.; Ben Sghaier, R.; Chaabouni, Y.; Msahli, S.; Sakli, F. Physico-chemical and mechanical characterization of alkali-treated *Agave americana* L. fiber. *J. Text. Inst.* **2012**, *103*, 349–355. [CrossRef]
28. Wang, X.; Chang, L.; Shi, X.; Wang, L. Effect of Hot-Alkali Treatment on the Structure Composition of Jute Fabrics and Mechanical Properties of Laminated Composites. *Materials* **2019**, *12*, 1386. [CrossRef] [PubMed]

29. Quiceno-Jaramillo, N. Efecto del Proceso de Mercerización en el Comportamiento de la Fibra de Hoja de Piña (FHP) como Refuerzo en Una Matriz de Polipropileno. Master's Thesis, Universidad Nacional de Colombia, Bogotá, Colombia, 2016.

30. Xie, Y.; Hill, C.A.S.; Xiao, Z.; Militz, H.; Mai, C. Silane coupling agents used for natural fiber/polymer composites: A review. *Compos. Part A Appl. Sci. Manuf.* **2010**, *41*, 806–819. [CrossRef]

31. Mondal, I.H.; Islam, K.; Ahmed, F. Effect of Silane Coupling Agents on Cotton Fibre Finishing. *J. Nat. Fibers* **2021**, *19*, 5451–5464. [CrossRef]

32. Hidalgo-Salazar, M.A.; Luna-Vera, F.; Correa-Aguirre, J.P. Biocomposites from Colombian Sugarcane Bagasse with Polypropylene: Mechanical, Thermal and Viscoelastic Properties. In *Characterizations of Some Composite Materials*; IntechOpen: London, UK, 2019; p. 13.

33. Correa-Aguirre, J.P.; Luna-Vera, F.; Caicedo, C.; Vera-Mondragón, B.; Hidalgo-Salazar, M.A. The Effects of Reprocessing and Fiber Treatments on the Properties of Polypropylene-Sugarcane Bagasse Biocomposites. *Polymers* **2020**, *12*, 1440. [CrossRef]

34. Luna-Vera, F.; Melo Cortes, H.A.; Murcia, C.V.; Charry-Galvis, I.C. Modificación superficial de micro fibras de celulosa obtenidas a partir de bagazo de caña de azúcar usando silanización. *Inf. Técnico* **2014**, *78*, 106–114.

35. Cappelletto, E.; Maggini, S.; Girardi, F.; Bochicchio, G.; Tessadri, B.; Di Maggio, R. Wood surface protection with different alkoxysilanes: A hydrophobic barrier. *Cellulose* **2012**, *20*, 3131–3141. [CrossRef]

36. Cisneros-López, E.O.; Pérez-Fonseca, A.A.; Fuentes-Talavera, F.J.; Anzaldo, J.; González-Núñez, R.; Rodrigue, D.; Robledo-Ortíz, J.R. Rotomolded polyethylene-agave fiber composites: Effect of fiber surface treatment on the mechanical properties. *Polym. Eng. Sci.* **2016**, *56*, 856–865. [CrossRef]

37. Sepe, R.; Bollino, F.; Boccarusso, L.; Caputo, F. Influence of chemical treatments on mechanical properties of hemp fiber reinforced composites. *Compos. Part B Eng.* **2018**, *133*, 210–217. [CrossRef]

38. Muñoz-Vélez, M.F.; Idalgo-Salazar, M.; Mina-Hernandez, J. Fibras de fique una alternativa para el reforzamiento de plásticos. Influencia de la modificación superficial. *Biotecnol. Sect. Agropecu. Agroindustrial* **2014**, *12*, 60–70.

39. Asumani, O.; Reid, R.; Paskaramoorthy, R. The effects of alkali–silane treatment on the tensile and flexural properties of short fibre non-woven kenaf reinforced polypropylene composites. *Compos. Part A Appl. Sci. Manuf.* **2012**, *43*, 1431–1440. [CrossRef]

40. Orue, A.; Jauregi, A.; Unsuain, U.; Labidi, J.; Eceiza, A.; Arbelaiz, A. The effect of alkaline and silane treatments on mechanical properties and breakage of sisal fibers and poly(lactic acid)/sisal fiber composites. *Compos. Part A Appl. Sci. Manuf.* **2016**, *84*, 186–195. [CrossRef]

41. Zhao, Y.; Qiu, J.; Feng, H.; Zhang, M. The interfacial modification of rice straw fiber reinforced poly(butylene succinate) composites: Effect of aminosilane with different alkoxy groups. *J. Appl. Polym. Sci.* **2012**, *125*, 3211–3220. [CrossRef]

42. Chauhan, V.; Kärki, T.; Varis, J. Effect of Fiber Content and Silane Treatment on the Mechanical Properties of Recycled Acrylonitrile-Butadiene-Styrene Fiber Composites. *Chemistry* **2021**, *3*, 1258–1270. [CrossRef]

43. Huda, M.S.; Drzal, L.T.; Mohanty, A.K.; Misra, M. Effect of fiber surface-treatments on the properties of laminated biocomposites from poly(lactic acid) (PLA) and kenaf fibers. *Compos. Sci. Technol.* **2008**, *68*, 424–432. [CrossRef]

44. Huang, Y.; Qian, S.; Zhou, J.; Chen, W.; Liu, T.; Yang, S.; Long, S.; Li, X. Achieving Swollen yet Strengthened Hydrogels by Reorganizing Multiphase Network Structure. *Adv. Funct. Mater.* **2023**, *33*, 2213549. [CrossRef]

45. Vieira, M.C.; Heinze, T.; Antonio-Cruz, R.; Mendoza-Martinez, A. Cellulose derivatives from cellulosic material isolated from Agave lechuguilla and fourcroydes. *Cellulose* **2002**, *9*, 203–212. [CrossRef]

46. Hashim, M.; Amin, A.; Faizan-Marwah, O.; Othman, M.; Yunus, M.; Huat, N. The effect of alkali treatment under various conditions on physical properties of kenaf fiber. *J. Phys. Conf. Ser.* **2017**, *914*, 012030. [CrossRef]

47. Sahu, P.; Gupta, M. A review on the properties of natural fibres and its bio-composites: Effect of alkali treatment. *Proc. Inst. Mech. Eng. Part L J. Mater. Des. Appl.* **2019**, *234*, 198–217. [CrossRef]

48. Teli, M.; Jadhav, A. Effect of Mercerization on the Properties of Pandanus Odorifer Lignocellulosic Fibre. *IOSR J. Polym. Text. Eng.* **2017**, *4*, 7–15. [CrossRef]

49. Jaramillo-Quiceno, N.; Vélez, J.M.; Cadena Ch, E.M.; Restrepo-Osorio, A.; Felipe Santa, J. Improvement of Mechanical Properties of Pineapple Leaf Fibers by Mercerization Process. *Fibers Polym.* **2018**, *19*, 2604–2611. [CrossRef]

50. Peña-Alonso, R.; Rubio, F.; Rubio, J.; Oteo, J.L. Study of the hydrolysis and condensation of γ-Aminopropyltriethoxysilane by FT-IR spectroscopy. *J. Mater. Sci.* **2006**, *42*, 595–603. [CrossRef]

51. Rubio, J.; Mazo, M.A.; Martín-Ilana, A.; Tamayo, A. FT-IR study of the hydrolysis and condensation of 3-(2-amino-ethylamino)propyl-trimethoxy silane. *Boletín Soc. Española Cerámica Vidr.* **2018**, *57*, 160–168. [CrossRef]

52. Le Moigne, N.; Longerey, M.; Taulemesse, J.-M.; Bénézet, J.-C.; Bergeret, A. Study of the interface in natural fibres reinforced poly(lactic acid) biocomposites modified by optimized organosilane treatments. *Ind. Crops Prod.* **2014**, *52*, 481–494. [CrossRef]

53. Lee, M.; Kim, Y.; Ryu, H.; Baeck, S.-H.; Shim, S.E. Effects of Silane Coupling Agent on the Mechanical and Thermal Properties of Silica/Polypropylene Composites. *Polym. Korea* **2017**, *41*, 599–609. [CrossRef]

54. Liu, L.; Yu, J.; Cheng, L.; Qu, W. Mechanical properties of poly(butylene succinate) (PBS) biocomposites reinforced with surface modified jute fibre. *Compos. Part A Appl. Sci. Manuf.* **2009**, *40*, 669–674. [CrossRef]

55. Perez-Pimienta, J.A.; Poggi-Varaldo, H.M.; Ponce-Noyola, T.; Ramos-Valdivia, A.C.; Chavez-Carvayar, J.A.; Stavila, V.; Simmons, B.A. Fractional pretreatment of raw and calcium oxalate-extracted agave bagasse using ionic liquid and alkaline hydrogen peroxide. *Biomass Bioenergy* **2016**, *91*, 48–55. [CrossRef]

56. De Dios Naranjo, C.; Alamilla-Beltrán, L.; Gutiérrez-Lopez, G.G.; Terres-Rojas, E.; Solorza-Feria, J.; Romero-Vargas, S.; Yee-Madeira, H.T.; Flores-Morales, A.; Mora-Escobedo, R. Isolation and characterization of cellulose obtained form Agave salmiana fibers using two acid-alkali extractipon methods. *Rev. Mex. Cienc. Agric.* **2016**, *7*, 31–43.
57. Asim, M.; Jawaid, M.; Abdan, K.; Nasir, M. Effect of Alkali treatments on physical and Mechanical strength of Pineapple leaf fibres. *IOP Conf. Ser. Mater. Sci. Eng.* **2018**, *290*, 012030. [CrossRef]
58. Wang, Q.; Zhang, Y.; Liang, W.; Wang, J.; Chen, Y. Effect of silane treatment on mechanical properties and thermal behavior of bamboo fibers reinforced polypropylene composites. *J. Eng. Fibers Fabr.* **2020**, *15*, 1558925020958195. [CrossRef]
59. Anna Dilfi, K.F.; Balan, A.; Bin, H.; Xian, G.; Thomas, S. Effect of surface modification of jute fiber on the mechanical properties and durability of jute fiber-reinforced epoxy composites. *Polym. Compos.* **2018**, *39*, E2519–E2528. [CrossRef]
60. Célino, A.; Fréour, S.; Jacquemin, F.; Casari, P. The hygroscopic behavior of plant fibers: A review. *Front. Chem.* **2014**, *1*, 43. [CrossRef] [PubMed]
61. Gogoi, R.; Tyagi, A.K. Surface Modification of Jute Fabric by Treating with Silane Coupling Agent for Reducing Its Moisture Regain Characteristics. *J. Nat. Fibers* **2021**, *18*, 803–812. [CrossRef]
62. García-Méndez, R.F.; Cortés-Martínez, C.I.; Almendárez-Camarillo, A. Thermochemical and Tensile Mechanical Properties of Fibers Mechanically Extracted from Leaves of *Agave angustifolia* Haw. *J. Nat. Fibers* **2022**, *19*, 3171–3185. [CrossRef]
63. Medellín-Castillo, N.; Hernández-Ramírez, M.; Salazar-Rábago, J.; Labrada-Delgado, G.; Aragón-Piña, A. Bioadsorción de plomo (ii) presente en solución acuosa sobre residuos de fibras naturales procedentes de la industria ixtlera (*Agave lechuguilla* Torr. Y *Yucca carnerosana* (Trel.) McKelvey). *Rev. Int. Contam. Ambient.* **2017**, *33*, 269–280. [CrossRef]
64. Muñoz, E.J.; Prieto-García, F.; Prieto-Méndez, J.; Acevedo-Sandoval, O.A.; Rodríguez-Laguna, R. Obtención de pulpa de celulosa a partir de residuos de *Agave salmiana* B. Otto ex Salm. Optimización. *DYNA* **2017**, *84*, 253–260. [CrossRef]
65. Balam-Cocom, R.J.; Duarte-Aranda, S.; Canché-Escamilla, G. Obtención y caracterización de materiales compuestos de fibras de la "piña" de henequén y polipropileno. *Rev. Mex. Ing. Quím.* **2006**, *5*, 39–44.
66. Márquez, A.; Cazaurang, N.; Gonzalez, I.; Colunga, P. Extraction of chemical cellulose from the fibers of *Agave lechuguilla* Torr. *Econ. Bot.* **1996**, *50*, 465–468. [CrossRef]
67. Munawar, S.S.; Umemura, K.; Kawai, S. Characterization of the morphological, physical, and mechanical properties of seven nonwood plant fiber bundles. *J. Wood Sci.* **2007**, *53*, 108–113. [CrossRef]
68. Ray, D.; Sarkar, B.K. Characterization of alkali-treated jute fibers for physical and mechanical properties. *J. Appl. Polym. Sci.* **2001**, *80*, 1013–1020. [CrossRef]
69. Krishnaiah, P.; Ratnam, C.T.; Manickam, S. Enhancements in crystallinity, thermal stability, tensile modulus and strength of sisal fibres and their PP composites induced by the synergistic effects of alkali and high intensity ultrasound (HIU) treatments. *Ultrason. Sonochem.* **2017**, *34*, 729–742. [CrossRef]
70. Borchani, K.E.; Carrot, C.; Jaziri, M. Untreated and alkali treated fibers from Alfa stem: Effect of alkali treatment on structural, morphological and thermal features. *Cellulose* **2015**, *22*, 1577–1589. [CrossRef]
71. Sawpan, M.A.; Pickering, K.L.; Fernyhough, A. Effect of various chemical treatments on the fibre structure and tensile properties of industrial hemp fibres. *Compos. Part A Appl. Sci. Manuf.* **2011**, *42*, 888–895. [CrossRef]
72. Vijay, R.; Singaravelu, D.L.; Vinod, A.; Sanjay, M.; Siengchin, S. Characterization of Alkali-Treated and Untreated Natural Fibers from the Stem of Parthenium Hysterophorus. *J. Nat. Fibers* **2019**, *18*, 80–90. [CrossRef]
73. Khanjanzadeh, H.; Behrooz, R.; Bahramifar, N.; Gindl-Altmutter, W.; Bacher, M.; Edler, M.; Griesser, T. Surface chemical functionalization of cellulose nanocrystals by 3-aminopropyltriethoxysilane. *Int. J. Biol. Macromol.* **2018**, *106*, 1288–1296. [CrossRef]
74. Abdelmouleh, M.; Boufi, S.; Belgacem, M.; Duarte, A.; Ben Salah, A.; Gandini, A. Modification of cellulosic fibres with function-alised silanes: Development of surface properties. *Int. J. Adhes. Adhes.* **2004**, *24*, 43–54. [CrossRef]
75. Valadez-Gonzalez, A.; Cervantes-Uc, J.; Olayo, R.; Herrera-Franco, P. Chemical modification of henequén fibers with an organosilane coupling agent. *Compos. Part B Eng.* **1999**, *30*, 321–331. [CrossRef]
76. Saha, P.K.; Mia, R.; Zhou, Y.; Ahmed, T. Functionalization of hydrophobic nonwoven cotton fabric for oil and water repellency. *SN Appl. Sci.* **2021**, *3*, 586. [CrossRef]
77. Zang, D.; Zhang, M.; Liu, F.; Wang, C. Superhydrophobic/superoleophilic corn straw fibers as effective oil sorbents for the recovery of spilled oil. *J. Chem. Technol. Biotechnol.* **2016**, *91*, 2449–2456. [CrossRef]
78. Majoul, N.; Aouida, S.; Bessaïs, B. Progress of porous silicon APTES-functionalization by FTIR investigations. *Appl. Surf. Sci.* **2015**, *331*, 388–391. [CrossRef]
79. Rao, X.; Hassan, A.A.; Guyon, C.; Zhang, M.; Ognier, S.; Tatoulian, M. Plasma Polymer Layers with Primary Amino Groups for Immobilization of Nano- and Microparticles. *Plasma Chem. Plasma Process.* **2020**, *40*, 589–606. [CrossRef]
80. Sundar, S.; Mariappan, R.; Piraman, S. Synthesis and characterization of amine modified magnetite nanoparticles as carriers of curcumin-anticancer drug. *Powder Technol.* **2014**, *266*, 321–328. [CrossRef]